Some Recent Developments in Flutter of Flat Panels

HERMAN L. BOHON* AND SIDNEY C. DIXON*
NASA Langley Research Center, Hampton, Va.

The accuracy of the two-dimensional static aerodynamic approximation for flutter analyses is investigated by comparison with results obtained on the basis of exact linearized three-dimensional potential flow theory. For unstressed panels, these results indicate that, for Mach numbers greater than 1.3, two-dimensional static aerodynamics is applicable over the whole range of length-width ratios greater than 1. The theoretical boundaries are also in good agreement with experimental data obtained from stress-free isotropic panels with length-width ratios from 1 to 10. For stressed panels, results using the approximate aerodynamics differ widely from the trends indicated by experiment; use of more exact aerodynamics does not alter this comparison, but inclusion of structural damping improves the correlation of theory and experiment. Experimental results for unstressed corrugation-stiffened panels are also presented and compared with theory. In some cases flutter occurred at dynamic pressures as low as 2% of the predicted value. An analysis of the effect of panel boundary conditions shows that such highly unconservative predictions may result from failure to account for the deflectional stiffness of the panel supports. Application of this analysis to the test panels results in marked improvement in the flutter predictions.

Nomenclature

$\bar{A}$ = flutter parameter defined by Eq. (A11)
A_m, B_m = constants of integration
a = panel length in x direction
$\bar{B}$ = frequency parameter defined by Eq. (A11)
b = panel width in y direction
C_0, C_1, C_2, C_3 = coefficient defined by Eqs. (A5)
D = flexural stiffness of isotropic panel
D_x = flexural stiffness of orthotropic panel in x direction
D_y = flexural stiffness of orthotropic panel in y direction
D_{xy} = twisting stiffness of orthotropic panel
D_1 = $D_x/(1 - \mu_x\mu_y)$
D_2 = $D_y/(1 - \mu_x\mu_y)$
F = complex amplitude of panel vibration, Eq. (A9)
g = structural damping coefficient
K = deflectional spring constant per unit width
$\bar{K}$ = spring-panel stiffness parameter, Eq. (B15)
M = Mach number
m = integer
N_x = inplane loading in x direction (positive in compression)
N_y = inplane loading in y direction (positive in compression)
$N_{x,\,cr}$ = critical inplane load
p = lateral loading
$\bar{p}$ = $\int_{-1/2}^{1/2} pY\,d\eta$
q = dynamic pressure of airstream
R = roots of characteristic equation, Eq. (B10)
r_1 = $\left(\frac{mb}{a}\right)^2\left(\frac{D_{xy}}{D_2} + \mu_x\right)$
r_2 = $\left(\frac{b}{a}\right)^4 \frac{D_1}{D_2}\left[\left(\frac{\omega}{\omega_r}\right)^2 - m^4\right]$
t = time
V = total potential energy of system
w = lateral deflection of panel
x, y = Cartesian coordinates of panel
Y = assumed function describing shape of flutter mode in y direction
Y_m = function describing shape of natural mode of vibration in y direction, Eq. (B16)
α, ϵ = roots of transcendental equation, Eq. (B13)
β = $(M^2 - 1)^{1/2}$
γ = mass per unit area of panel
η = y/b
λ = $2qa^3/\beta D_1$
μ_x, μ_y = Poisson's ratio associated with curvature in y and x directions, respectively
ξ = x/a
φ = parameter defined by Eq. (B17)
ψ = parameter defined by Eq. (B15)
ω = circular frequency
ω_r = $\frac{\pi^2}{a^2}\left(\frac{D_1}{\gamma}\right)^{1/2}$

Introduction

PANEL flutter is a self-excited oscillation of the external surface skin of a flight vehicle which results from the dynamic instability of the aerodynamic, inertial, and elastic forces of the system. This type of instability was supposedly first encountered in flight by the German V-2 missiles[1] and was considered to be the cause of several failures. During the 1950's, several experimental investigations were conducted to verify the existence of panel flutter and to determine some of the effects of such parameters as panel length-width ratio, thickness, and differential pressure.[1,2] During this same period, panel flutter was the subject of numerous theoretical investigations that, for the most part, were restricted to semi-infinite panels or panels on many supports.[3–6] Hedgepeth's[7] application of the two-dimensional static aerodynamic approximation to the panel flutter problem greatly simplified the analytical complexities and resulted in a differential equation that can be solved exactly for finite panels. Comprehensive reviews of both theoretical and experimental panel flutter investigations conducted prior to 1960 have been published by Fung[8] and Stocker.[9]

During the period preceding 1960, panel flutter had been considered more or less an academic problem of little practical significance. However, during 1959, wind-tunnel tests indicated that certain structural components of the X-15 airplane were susceptible to panel flutter.[10, 11] These reports were followed by a published compilation[12] of flight flutter results for existing aircraft which indicated that panel flutter

Presented at the AIAA Fifth Annual Structures and Materials Conference, Palm Springs, Calif., April 1–3, 1964 (no preprint number; published in bound volume of preprints of the meeting); revision received August 24, 1964.

* Aerospace Engineer.

had become a significant structural problem in the design of supersonic vehicles.

The emergence of panel flutter as a significant structural problem caused the generation of considerable experimental and theoretical research. A partial bibliography of these investigations is given in the references.[13-26] Although the variety of configurations studied experimentally were seldom representative of the idealized conditions imposed by theory, these studies have revealed major differences between experiment and theory for both stressed isotropic panels[25] and unstressed corrugation-stiffened panels.[26] In addition, a third area of concern is flutter of long narrow panels for which it is generally thought that more refined aerodynamic theories are necessary to predict flutter results accurately. It is the purpose of this paper to determine whether flutter results utilizing two-dimensional static aerodynamics are applicable to long narrow panels and also to examine reasons for the apparent differences between theory and experiment for stressed isotropic panels and unstressed corrugation-stiffened panels.

In order to assess the accuracy of the theory using two-dimensional static aerodynamics and to determine its range of validity, a simply supported isotropic panel has been investigated in both the stressed and unstressed conditions. Calculated flutter results utilizing the simpler two-dimensional aerodynamics are compared with results obtained from an analysis by Cunningham[27] which utilizes three-dimensional unsteady aerodynamics (hereafter referred to as exact aerodynamics).

For unstressed panels, the comparison is used to examine the range of Mach number M and length-width ratio a/b for which the simpler aerodynamic approximation gives reasonable results for simply supported isotropic panels. Since considerable attention has previously been given to the range of $a/b < 1$, and since other factors such as boundary layer appear to be important in this range,[28, 29] numerical results will be presented only for the range $a/b \geqq 1$. It will be shown that for $M \geqq 1.3$ the approximate aerodynamic theory is in good agreement with the exact aerodynamic theory. In addition, it is shown that theory is in reasonable agreement with experiment for unstressed isotropic panels.

For stressed isotropic panels, experiment indicates that the most critical portion of the flutter boundary occurs at the transition from the flat unbuckled boundary to the postbuckled boundary.[17] However, theoretical results based on the approximate aerodynamics indicate that the most critical condition for flutter can occur at values of midplane load considerably less than that required for buckling.[22, 25] It has been suggested that this discrepancy is due to the use of the static aerodynamics.[25] A flutter analysis of a stressed panel utilizing the exact aerodynamics is made, and it is found that, although damping has a pronounced effect, the exact aerodynamics does not completely eliminate the apparent discrepancies.

In addition, experimental and theoretical results for corrugation-stiffened panels are presented. It is shown that the orthotropic plate equation should give flutter results in reasonable agreement with experiment for unstressed panels. However, test results for corrugation-stiffened panels indicate that in some cases flutter occurred at dynamic pressures as low as 2% of the theoretical value for a simply supported panel. This large discrepancy is attributed to the improper representation in the theory of the flexibility of the edge supports at the ends of the corrugations. Analyses are presented to show that because of the stiffness properties of a corrugation-stiffened panel, the deflectional flexibility of the edge attachments can greatly affect the flutter characteristics. An approximate flutter analysis of this effect is presented, and for a reasonable estimate of the edge flexibility for the experimental panels, experiment and theory are found to be in fair agreement.

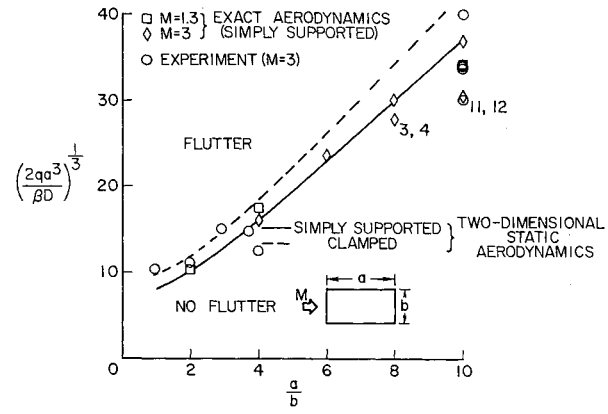

Fig. 1 Theoretical and experimental flutter results for flat isotropic rectangular panels with no midplane stress.

Comparison of Flutter Results from Approximate and Exact Aerodynamics

Hedgepeth's paper[7] utilizing two-dimensional static aerodynamics made several comparisons with results obtained from more refined aerodynamics. He found good agreement between the results for two-dimensional (strip theory) and three-dimensional (surface theory) static aerodynamics when $\beta(b/a) \geqq 1$; he did not consider the case for $\beta(b/a) < 1$. He also compared his results with the results of a two-mode analysis that took into account unsteady effects for both the two- and three-dimensional theories for values of a/b of 0 and 1. The results based on unsteady aerodynamics agreed well with the results based on the static approximation for values of M greater than somewhere between $(2)^{1/2}$ and 2. The results based on three-dimensional unsteady aerodynamics were for an array of panels.

The flutter analysis recently formulated by Cunningham[27] permits investigation of single finite panels using exact three-dimensional unsteady aerodynamics. Because of the complexity of the problem, the analysis is of the modal type requiring high-speed computing machines. In this paper the exact aerodynamics is employed to examine the useful range in Mach number and length-width ratio (for $a/b \geqq 1$) of the closed-form solution based on two-dimensional static aerodynamics for unstressed panels. In addition, a flutter analysis is made to determine whether the use of exact aerodynamics alters the trends indicated by the two-dimensional static aerodynamic approximation for stressed panels.

Unstressed Panels

Some theoretical and experimental results for flat rectangular panels are shown in Fig. 1 in terms of the panel flutter parameter $(2qa^3/\beta D)^{1/3}$ and the panel length-width ratio a/b. The panels are stress free, and the flow is as indicated in this figure. The solid curve represents the flutter boundary for panels simply supported on all edges, as given by Hedgepeth's[7] closed-form solution of the differential equation based on two-dimensional static aerodynamics. The dashed curve represents the flutter boundary obtained from an analysis by Houbolt[30] utilizing the same aerodynamic approximation for panels clamped on all edges. The square symbols represent flutter points calculated by Cunningham[27] for simply supported aluminum-alloy panels at sea level for a Mach number of 1.3. The diamond symbols represent flutter points obtained by Cunningham's method for the same panels but at a Mach number of 3.0.

The results of the closed-form solution, based on the approximate aerodynamics, show that for unstressed panels the critical flutter boundary always results from the coalescence of the frequencies of the two lowest natural modes of vibration. The unlabeled diamond symbols shown in Fig. 1 also

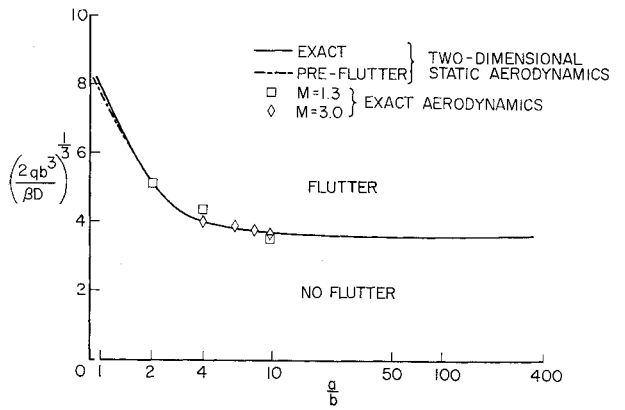

Fig. 2 Variation of $(2qb^3/\beta D)^{1/3}$ with a/b obtained from both exact and two-dimensional static aerodynamics for simply supported rectangular panels with no midplane stress.

correspond to a "mode 2,1" boundary. (In this discussion, the flutter boundaries obtained from the exact aerodynamics will be described by reference to the two most predominant vibration modes in the flutter mode shape.) For $a/b > 6$ the exact aerodynamics indicated that higher-mode boundaries could become the critical boundaries, as indicated at $a/b = 8$ and 10 by the labeled diamond points. (The subscripts indicate the dominant modes.) However, it is felt that this result is attributable to nonconvergence of the solution. At present, Cunningham's method is programed for computation at the NASA Langley Research Center so as to employ a maximum of 12 modes. Thus, for example, a "mode 11, 12" boundary would not be expected to converge fully, whereas a "mode 2, 1" boundary would be more nearly converged. When less than 12 modes were used in the analysis, the flutter boundaries were raised as the number of modes used in the analysis was increased. Calculations were made for a/b of 10 using modes 3 through 14. These calculations raised the "mode 11, 12" boundary considerably and probably resulted in a more converged solution. In addition, Hedgepeth has shown for the approximate aerodynamics that, when an insufficient number of modes is used in the analysis, the resulting flutter boundary is lower than the boundary obtained from the closed-form solution (provided an even number of modes is used). For these reasons it was felt that the "mode 2, 1" boundary results (the unlabeled diamonds) at a/b of 8 and 10 more nearly represent the converged solution.

For $a/b \leqq 6$, the modal solution, based on the exact aerodynamics, is considered to be well converged. For this range of a/b, the results obtained from Hedgepeth's solution are in excellent agreement with the flutter results obtained using exact aerodynamics. The differences in the results given by the exact and approximate aerodynamic theories are considered to be a measure of the three-dimensional and unsteady effects. At a/b of 4 (Fig. 1) the exact aerodynamics indicates a variation of $(2qa^3/\beta D)^{1/3}$ of approximately 7% as M is varied from 1.3 to 3, with the results obtained for $M = 3$ essentially identical to the results obtained from the closed-form solution. Thus, the three-dimensional and unsteady effects are seen to be small. However, some unpublished results obtained by Cunningham for a/b of 1 (not shown in Fig. 1) indicate a variation of $(2qa^3/\beta D)^{1/3}$ of approximately 30% as M is varied from 1.3 to 3; again the results for $M = 3$ are essentially identical to the results obtained from the closed-form solution. Hence, it may be expected that the three-dimensional and unsteady effects are important in the low Mach number range for $a/b \leqq 1$. The Mach number effect given by the approximate aerodynamic theory is, of course, accounted for only by the ordinate parameter.

For $a/b \geqq 6$ the results obtained from the closed-form solution are also in excellent agreement with the "mode 2, 1" results shown from the exact aerodynamic theory. Although the question of convergence of the solutions exists, even the lowest of the other boundaries obtained from the exact aerodynamics were also in fair agreement with the closed-form solution, differing at most by 8% at a/b of 8 ("mode 3, 4" boundary) and 18% at a/b of 10 ("mode 11, 12" boundary). Hence, at least fair numerical agreement is shown for M as low as 1.3 and a/b as large as 10 (or $\beta(b/a)$ of 0.083).

The circles in Fig. 1 represent published[17–21] and unpublished experimental flutter points for isotropic panels obtained at a Mach number of 3.0. The experimental data shown are for essentially flat panels tested under aerodynamic heating conditions. In general, these points were obtained from tests that involved thermal midplane stresses, but data were obtained sufficiently close to zero thermal stress that an extrapolation could be made to get essentially zero stress flutter points. The data shown are for clamped edges and edges intermediately between simply supported and clamped. The scatter in the data shown is probably due in part to difficulties in extrapolating to zero stress points. Such scatter is fairly typical of panel flutter experiments when data are obtained from a variety of configurations. However, considering the entire range of a/b from 1 to 10, the agreement between theory and experiment must be considered reasonable.

It would be difficult to determine from Fig. 1 the trend of the results for $a/b > 10$. A better insight can be obtained by redefining the flutter parameter in terms of the panel width instead of length and plotting this parameter $(2qb^3/\beta D)^{1/3}$ as a function of a/b, as is shown in Fig. 2.

The solid curve is the boundary obtained from Hedgepeth's closed-form solution of the governing differential equation and indicates that the dynamic pressure for flutter is essentially independent of length for $a/b > 10$. Calculations from exact aerodynamics (indicated by the square and diamond symbols) suggest the same thing; hence, it would appear that for $M \geqq 1.3$, two-dimensional static aerodynamics is applicable for any unstressed panel over the entire range $a/b > 1$.

Figure 2 also illustrates the validity of a useful simplified method for the calculation of the flutter parameter. Movchan[31] pointed out a solution to the differential equation which corresponds to a natural mode of vibration under airflow where the motion is stable. That is, the airflow corresponds to a speed less than the flutter speed. This solution, which is referred to as the "preflutter" solution, leads to the following simple algebraic equation rather than the complex transcendental equation required for the complete solution

$$\frac{2qa^3}{\beta D} = \frac{4}{3}\pi^3(10 - \bar{A})\left(\frac{4 - \bar{A}}{6}\right)^{1/2} \tag{1}$$

where, for simply supported isotropic stress-free panels,

$$\bar{A} = -2(a/b)^2$$

Results from Eq. (1) are shown by the dot-dashed curve in Fig. 2, which is in very close agreement with Hedgepeth's solution; in fact, for $a/b > 2$, the two virtually coincide. Thus, for the range of M and a/b for which two-dimensional static aerodynamic theory is valid, the critical value of the flutter parameter for unstressed isotropic panels can be readily obtained from Eq. (1). Based on the comparison of theory with experiment shown in Fig. 1, the results so obtained should be fairly accurate.

Stressed Panels

The results just presented suggest that the trends obtained from analyses utilizing two-dimensional static aerodynamics are essentially correct, particularly for moderate values of

a/b and large values of M. However, it appears that for stressed panels the theoretical trends are often not correct. For example, it has been shown[25] that for no damping, two-dimensional static aerodynamics predicts zero dynamic pressure required for flutter of stressed panels whenever the compressive midplane load has caused the two lowest panel vibration frequencies to be equal. In addition, the theory indicates changes in flutter mode as the compressive load increases, although such changes have not been observed experimentally. Although the inclusion of aerodynamic and structural damping removes the zero dynamic pressure points, the over-all trends are otherwise unaltered. On the other hand, experimental flutter boundaries[17–21] display none of the anomalous behavior associated with coincidence of the theoretical frequencies. It has been suggested that this discrepancy between theory and experiment for stressed panels is due primarily to the use of static aerodynamics.[25] Thus, it would be interesting to consider some results for stressed panels based on exact aerodynamics which, of course, includes the unsteady effects.

Figure 3 shows theoretical results obtained from both the two-dimensional static and exact aerodynamics for a simply supported panel. The panel length-width ratio is 4 and $N_y = 0$. The exact aerodynamics results were obtained from a six-mode solution and are based on aluminum-alloy panels at sea level at $M = 3.0$; this value of M corresponds to the value at which most published experimental data for stressed panels have been obtained. The results are presented in terms of the flutter parameter $(2qa^3/\beta D)^{1/3}$ and the ratio of the midplane compressive load to the critical value required for buckling $N_x/N_{x,cr}$. The solid curve represents the results obtained from Hedgepeth's solution based on the approximate aerodynamic theory; the numbers on the curve indicate the modes that coalesced for flutter. As can be seen from Fig. 3, zero values of the flutter parameter occur at values of $N_x/N_{x,cr}$ of approximately 0.58, 0.71, and 0.89, and the flutter mode changes from a combination of modes 1 and 2 to a combination of modes 3 and 4.

The circles on Fig. 3 represent flutter points obtained from exact aerodynamics for no structural damping. As can be seen, these results are in excellent quantitative agreement with the results based on the approximate aerodynamic theory, except near the critical values of $N_x/N_{x,cr}$ where the aerodynamic damping, which is included in the exact theory, tended to eliminate the zero-dynamic-pressure flutter points. The exact aerodynamics also indicated changes in flutter mode similar to the changes given by the closed-form solution. Thus, the use of exact aerodynamics has little effect on the differences between theory and experiment for flutter of stressed panels. The dashed and dot-dashed curves shown in Fig. 3 represent results obtained from the exact aerodynamics for values of the structural damping coefficient of 0.01 and 0.025, respectively. As can be seen, structural damping also has a large effect near regions where the approximate aerodynamics predicts zero values of the flutter dynamic pressure. This same trend was observed for the approximate aerodynamic theory when damping was added to the analysis.[25] The inclusion of damping in the analysis tends to smooth out the saw-toothed-like boundary ($N_x/N_{x,cr} > 0.5$), and the resulting flutter trends might be considered to be in qualitative agreement with existing experimental boundaries. However, the large values of damping necessary to obtain this agreement suggest that other factors, such as boundary layer, differential pressure, and initial imperfections must be considered if the discrepancies are to be removed.

It should be pointed out that most experimental investigations of stressed panels did not include measurements or control of the boundary layer or initial imperfections and considered differential pressure in an approximate manner, if at all. In addition, the panels were usually subjected to nonuniform temperature increases and the stress distributions are imperfectly known, at best. Thus, a need for more refined experimental data to serve as a guide for future theoretical investigations is obvious.

Flutter Results for Orthotropic Panels

The use of orthotropic panels, and, in particular, corrugation-stiffened panels, has had widespread application in design of exposed skin components of supersonic and re-entry types of vehicles. Although the general practice of orienting the corrugations normal to the airstream results in a panel much more susceptible to flutter than the same panel with corrugations in the direction of the stream, the flutter dynamic pressure given by theory may still be considerably greater than that for an isotropic panel of equal weight. However, it will be shown below by recent experimental results for corrugation-stiffened panels that direct application of conventional theory gives highly unconservative results. Since the results reported in the foregoing indicate that the approximate aerodynamics of the conventional theory probably does not account for this discrepancy, another potential reason will be considered in some detail.

Comparison of Theory and Experiment

As was noted previously, application of Cunningham's[27] flutter solution using exact aerodynamics (see Fig. 1) revealed that two-dimensional static aerodynamics is useful over a much greater range of length-width ratio than was previously expected. It was also shown that for negative values of $\bar{A}$, Movchan's[31] preflutter solution predicts the flutter speed adequately (see Fig. 2). Thus, since corrugation-stiffened panels are represented by large negative values of $\bar{A}$, Movchan's solution will be used for comparison with experiment.

Some recent experimental data are compared with the preflutter solution in Fig. 4 on a plot of the dynamic-pressure parameter $(2qa^3/\beta D_1)^{1/3}$ and the stiffness parameter $\bar{A}$. The theoretical results for orthotropic panels can be shown[16] to be the same as for isotropic panels if D is replaced by D_1 (the streamwise flexural stiffness) in the ordinate parameter and the stiffness ratio D_{xy}/D_1 is used in the abscissa parameter.

The curve is the theoretical flutter boundary based on the preflutter solution for simply supported edges. The symbols represent experimental flutter results for unstressed panels. The diamond symbol is a flutter point for a square corrugation-stiffened panel tested at a Mach number of 1.87.[32] The two square symbols represent data on corrugation-stiffened panels with geometric length-width ratios of 1.5 and 10 obtained from wind-tunnel tests at Mach 3 on the full-scale X-15 vertical stabilizer.[11] The other symbols represent

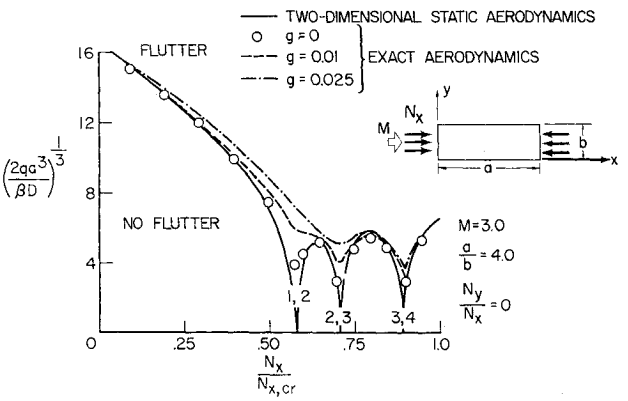

Fig. 3 Comparison of results obtained from exact and two-dimensional static aerodynamics for flat panel subjected to midplane compressive load.

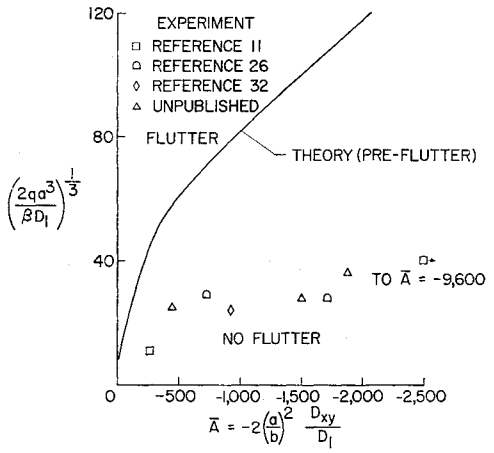

Fig. 4 Comparison of theory using static aerodynamics and experiment for flat unstressed corrugation-stiffened panels ($\mu_x = 0$).

published[26] and unpublished data obtained from corrugation-stiffened panels at Mach number 3.0 with length-width ratios of 1.0. As can be seen, the theoretical predictions for orthotropic panels are highly unconservative; the difference between theory and experiment increases rapidly as $\bar{A}$ increases negatively.

The large discrepancies shown probably cannot be explained on the basis of a single parameter. It appears now, however, that the exact aerodynamics will not eliminate the problem. Further, the panel stiffnesses D_1, D_2, and D_{xy} are believed to be known adequately. These stiffnesses were calculated by the method developed by Stroud[33] in which experimental verification of the theoretical results is shown. Inclusion of the effects of finite transverse shear stiffness has been shown[13] to have a significant effect on the flutter predictions if shear deflections are important compared with bending deflections. However, preliminary calculations of these stiffnesses for the panels represented in Fig. 4 indicated that shear deflections would not be significant and, thus, theory that neglects transverse shear stiffness should be valid.

The large discrepancies between theory and experiment may, however, be explained by the differences between the idealized boundary conditions assumed in the theory and the actual edge restraint imposed by the panel supports. Because of the nature of the construction of corrugation-stiffened panels, the corrugations seldom extend the full width of the panel, and the entire cross section is not firmly anchored at the support. In practice, attachment of the edges of corrugation-stiffened panels may be similar to those illustrated in Fig. 5a where the corrugations hang freely at the edge (open end) or are crushed to the flat outer skin (closed end). Usually the attachment to the support is made only through one or two sheet thicknesses and, thus,

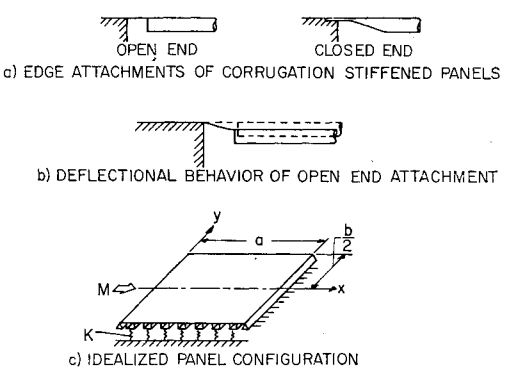

Fig. 5 Actual and idealized edge attachment for corrugation-stiffened flutter panels.

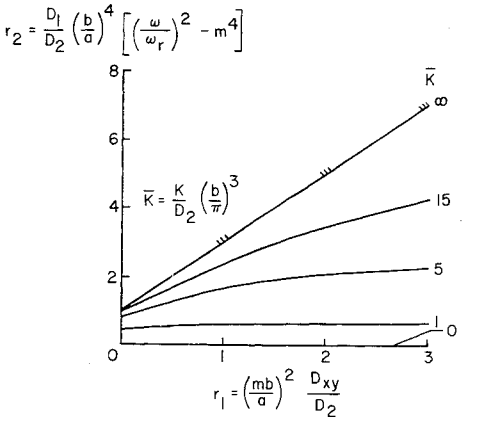

Fig. 6 Exact vibration frequencies for orthotropic panel simply supported on two edges as a function of deflectional spring stiffness ($\mu_x = 0$).

the panel can experience localized deflections in the vicinity of the edges in a manner similar to that indicated in Fig. 5b. Therefore, instead of zero deflection at the edge, the panel can be considered to be attached to deflectional springs with stiffnesses that may be quite small compared with the maximum flexural stiffness D_2 of the panel. The idealized panel configuration shown in Fig. 5c (simply supported on the leading and trailing edges and supported by deflectional springs on the other two edges) is analyzed for flutter and discussed in the following sections.

Effects of Deflectional Spring Supports

Analysis

In Appendix A the method of Kantorovich[34] is employed to obtain the governing differential equation and boundary conditions for flutter of orthotropic panels simply supported on the leading and trailing edges and supported by deflectional springs along the streamwise edges. The method involves the assumption of a cross-stream mode shape that is integrated over the panel width. Thus, the coefficients of the resulting ordinary differential equation [Eq. (A10)] are functions of the assumed cross-stream mode shape [see Eqs. (A5)]. This differential equation, which can be solved exactly, describes the problem in an approximate manner and is correct only when the edges parallel to the airflow are simply supported. However, satisfactory solutions can be obtained for other boundary conditions, provided that the assumed mode shape is a good approximation to the actual deflection. The cross-stream mode shapes used herein were obtained from the natural vibration modes of the panel which are calculated in Appendix B.

The results of the vibration analysis can also be used to give further insight into the flutter characteristics of orthotropic panels supported on deflectional springs. The vibration frequencies for modes having one half-wave in the y direction and m half-waves in the x direction are shown in Fig. 6 as a function of the panel stiffness for various values of the spring stiffness. The curves shown were obtained upon solution of the transcendental equation (B14) of Appendix B. The line for an infinite spring stiffness ($\bar{K} = \infty$) gives the frequencies for a panel simply supported on all edges. As $\bar{K}$ takes on smaller finite values, the panel frequencies are seen to decrease rapidly; for $\bar{K} = 0$ (lateral edges completely free) the solution reduces to (neglecting Poisson's effect) that for a simply supported beam of stiffness D_1. As can be seen from the figure, for small values of the spring stiffness ($\bar{K} \approx 1$, which is typical of some of the panels tested) the panel approaches the vibration behavior of a beam. This result may have a very pronounced effect on the flutter characteristics of corrugation-stiffened panels

oriented such that the flexural stiffness D_2 is greater than D_1 or, in general, for panels having large negative values of $\bar{A}$. That such is the case can be illustrated by an example from Fig. 4. Consider a square simply supported ($\bar{K} = \infty$) panel at $\bar{A} = -1500$; the predicted flutter parameter is $(2qa^3/\beta D_1)^{1/3} = 95$. It can be shown that a beam is represented by $\bar{A} = 0$. Thus, this same panel, if it were not supported along the edges ($\bar{K} = 0$), would have a value of the flutter parameter $(2qa^3/\beta D_1)^{1/3} = 7$. In other words, if $\bar{K}$ is small enough that the panel behavior is more like a beam than a simply supported panel, there can result a change of several orders of magnitude in dynamic pressure required for flutter. However, for a geometrically similar ($a/b = 1$) isotropic panel, $\bar{A} = -2$ when $\bar{K} = \infty$, and the difference between the result for a beam and the result for a simply supported panel is relatively small.

Theoretical flutter results and comparison with experiment

Theoretical flutter results are corrected for finite deflectional springs, as shown in Appendix A. The solution is seen to be identical to that for an isotropic panel, provided the parameter $\bar{A}$ is redefined according to Eq. (A11). For the case of zero stress, $\bar{A}$ is given by (neglecting Poisson's ratio)

$$\bar{A} = -2\left(\frac{a}{b}\right)^2 \frac{C_3}{\pi^2 C_0} \frac{D_{xy}}{D_1} \tag{2}$$

The coefficient $C_3/\pi^2 C_0$ is a function of the mode shape as indicated in Eq. (A5); for the natural vibration modes derived in Appendix B, $C_3/\pi^2 C_0$ varies with the spring stiffness parameter $\bar{K}$, as indicated in Fig. 7. As $\bar{K}$ approaches ∞, $C_3/\pi^2 C_0$ approaches 1, and $\bar{A}$ corresponds to a simply supported plate; if there is no support at the lateral edges ($\bar{K} = 0$), $C_3/\pi^2 C_0$ is zero, and $\bar{A}$ is then zero corresponding to a beam.

From Fig. 7 it can be seen that, in order to apply the results to panels having intermediate values of $\bar{K}$, it is necessary to specify an additional parameter $[m(b/a)]^2(D_{xy}/D_2)$ where m is the longitudinal mode number in the vibration analysis. It seems reasonable to pick a mode number m corresponding to the mode that contributes most to the deflection of the flutter mode. This mode number was considered to be that nearest twice the panel length-width ratio, such that the parameter $[m(b/a)] = 2$.

The results of the analysis of the deflectional spring effect have been applied to the experimental data from Fig. 4 and are shown in Fig. 8; note that the abscissa parameter $\bar{A}$ now contains the coefficient $C_3/\pi^2 C_0$. The open symbols represent the location of the experimental data if all panel edges were simply supported (that is, if $C_3/\pi^2 C_0 = 1.0$). The solid symbols with the band represent the approximate locations of the data when the deflectional spring effect is taken into account. Unfortunately, the experimental investigations were not conducted to evaluate the effects of deflectional springsupports and, thus, the actual spring constants for the test panels were not measured nor amenable to simple calculations. The method used to calculate $\bar{K}$ accounts for the reduction in flexural stiffness D_2 near the supports as well as the flexibility of the supports. It is felt that the assumptions employed in the spring calculations yield values of $\bar{K}$ probably greater than actual values; therefore, a minimum value for $\bar{K}$ was chosen arbitrarily as one-half the calculated $\bar{K}$. Use of these two values of $\bar{K}$ and the parameter $[m(b/a)] = 2$ allows the test results to be plotted as a band covering a range of $\bar{A}$. It is worth noting that, prior to the flutter tests, frequency measurements were obtained for the first few modes of two of the test panels. Plotting these measured frequencies on Fig. 6 indicated corresponding values of $\bar{K}$ reasonably close to the calculated values.

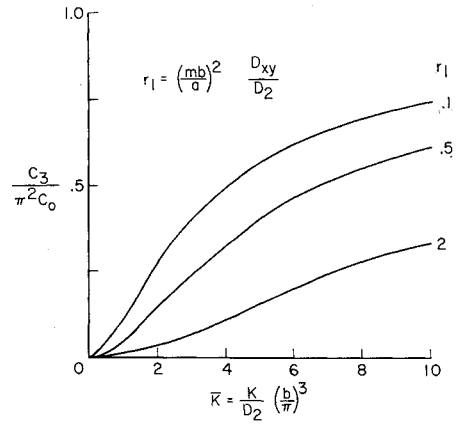

Fig. 7 Effect of deflectional spring on panel flutter coefficient $C_3/\pi^2 C_o$ for various values of r_1 ($\mu_x = 0$).

The salient fact is that the effect of finite deflectional spring stiffness along the panel edges is so significant that portions of the experimental band now lie reasonably close to theory. Thus, although more careful determination of support stiffness and, perhaps, a more exact analysis would have to be made to obtain the true effect, it may be concluded that prediction of the flutter characteristics of orthotropic panels requires careful consideration of the edge attachments and supports.

Concluding Remarks

Results obtained from panel flutter theory utilizing exact aerodynamics are compared with results obtained from theory employing two-dimensional static aerodynamics. This comparison revealed that the flutter boundary for unstressed rectangular isotropic panels obtained from the simpler aerodynamic theory agreed well with the results based on exact aerodynamics for Mach numbers $M \geqq 1.3$ and values of the panel length-width ratio a/b from 1 to 10. Both theories suggest that the flutter dynamic pressure is essentially independent of length for $a/b > 10$. Thus, the approximate aerodynamics appears applicable for $M \geqq 1.3$ for the entire range of $a/b > 1.0$. Although exact solutions based on the approximate aerodynamics still require considerable effort, Movchan's preflutter solution is shown to give essentially the same results with a tremendous saving in effort. The preflutter solution yields a simple algebraic expression for the critical flutter dynamic pressure. The theoretical boundaries were in reasonable agreement with experimental data obtained from stress-free isotropic panels over the range of a/b from 1 to 10.

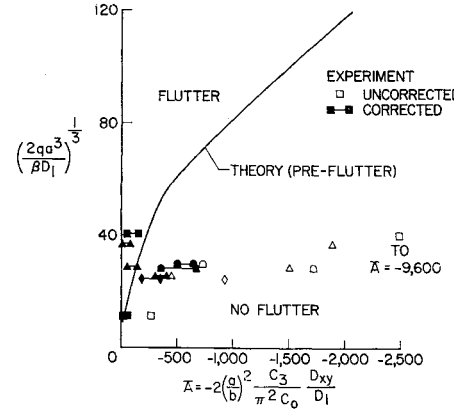

Fig. 8 Comparison of theory with experimental data for corrugation-stiffened panels when corrected for deflectional spring stiffness ($\mu_x = 0$).

Application of the exact aerodynamics to the flutter of stressed isotropic panels yielded results similar to those obtained from theory based on the two-dimensional static aerodynamics. The results indicated trends that differ from the trends shown by experiment. Although damping tended to remove the differences between theory and experiment, it appears that other factors (for example, differential pressure, initial imperfections, etc.) must be considered if the discrepancies are to be removed.

In contrast to the results for isotropic panels, experimental data presented for stress-free orthotropic (corrugation-stiffened) panels were as low as 2% of the theoretical predictions for simply supported panels. This large discrepancy was attributed primarily to the use in the theory of the idealized edge attachment normal to the corrugations. A vibration analysis was made on orthotropic panels supported by deflectional springs along edges normal to the corrugations. This analysis showed that for small values of spring stiffness the orthotropic panel behaved more like a beam than a plate. Such characteristics are shown to reduce greatly the dynamic pressure for flutter The experimental data for the corrugation-stiffened panels, corrected for calculated values of the deflectional spring stiffnesses of the test panels, showed marked improvement in comparison with theory. These results indicate that careful consideration of edge attachments of orthotropic panels is required for reliable flutter predictions.

Appendix A: Flutter Analysis of Orthotropic Panels on Deflectional Spring Supports

A method commonly employed for a flutter analysis of flat, finite panels consists of assuming a deflection function as the product of a known function that satisfies the boundary conditions on two opposite edges and an unknown function, and then applying the Galerkin procedure to reduce the partial differential equation to an ordinary differential equation in the unknown function.[25, 30] The ordinary differential equation may then be solved directly for flutter. However, if the edges of the panel are permitted to deflect, a product solution cannot satisfy the boundary conditions. Therefore, application of a Galerkin procedure may not be valid unless special attention is given to the solution at the boundaries. For this case a more direct approach to the ordinary differential equation can be made by applying the method of Kantorovich,[34] which starts with the expression for the potential energy of the system. This method will be used in the following analysis for an orthotropic plate.

Consider the panel, shown in Fig. 5c, simply supported on two opposite edges and supported by deflectional springs of stiffness K on the other two edges. The panel has a length a and width b and is subjected to inplane loads N_x and N_y and a lateral load p. The total potential energy of the system is written, in terms of orthotropic plate properties, as[35]:

$$V = \frac{1}{2}\int_0^a\int_{-b/2}^{b/2}\left[D_1\left(\frac{\partial^2 w}{\partial x^2}\right)^2 + 2\mu_y D_1\frac{\partial^2 w}{\partial x^2}\frac{\partial^2 w}{\partial y^2} + D_2\left(\frac{\partial^2 w}{\partial y^2}\right)^2 + 2D_{xy}\left(\frac{\partial^2 w}{\partial x\,\partial y}\right)^2 - 2pw - N_x\left(\frac{\partial w}{\partial x}\right)^2 - N_y\left(\frac{\partial w}{\partial y}\right)^2\right]dy\,dx + \frac{1}{2}\int_0^a Kw^2|_{b/2}\,dx + \frac{1}{2}\int_0^a Kw^2|_{-b/2}\,dx \quad \text{(A1)}$$

where

$$\left.\begin{aligned} D_1 &= D_x/(1-\mu_x\mu_y)\\ D_2 &= D_y/(1-\mu_x\mu_y)\\ \mu_x D_2 &= \mu_y D_1 \end{aligned}\right\} \quad \text{(A2)}$$

If the deflection is assumed to be given by

$$w = Y(\eta)F(\xi) \quad \text{(A3)}$$

where Y is a known function and $\eta = y/b$ and $\xi = x/a$, the problem is to find the function F which renders V a minimum. Substituting (A3) into (A1) and integrating with respect to η gives the potential energy as

$$V = \frac{ab}{2}\int_0^1\left[\frac{D_1C_0}{a^4}(F'')^2 + \frac{2\mu_y D_1C_1}{a^2b^2}FF'' + \left(\frac{D_2C_2}{b^4} - \frac{N_y}{b^2}C_3\right)F^2 + \left(\frac{2D_{xy}C_3}{a^2b^2} - \frac{N_x}{a^2}C_0\right)(F')^2 - 2\bar{p}F\right]d\xi + \frac{a}{2}\int_0^1 K\left[Y^2\left(\frac{1}{2}\right) + Y^2\left(-\frac{1}{2}\right)\right]F^2 d\xi \quad \text{(A4)}$$

where

$$\left.\begin{aligned} C_0 &= \int_{-1/2}^{1/2} Y^2 d\eta & C_3 &= \int_{-1/2}^{1/2}(Y')^2 d\eta\\ C_1 &= \int_{-1/2}^{1/2} YY''d\eta & \bar{p} &= \int_{-1/2}^{1/2} pY\,d\eta\\ C_2 &= \int_{-1/2}^{1/2}(Y'')^2 d\eta \end{aligned}\right\} \quad \text{(A5)}$$

The primes denote differentiation with respect to η or ξ. Application of the calculus of variations to Eq. (A4) leads to the following differential equation on the function F:

$$F^{IV} + \left[\frac{a^2N_x}{D_1} - 2\left(\frac{a}{b}\right)^2\frac{D_{xy}}{D_1}\frac{C_3}{C_0} + 2\mu_y\left(\frac{a}{b}\right)^2\frac{C_1}{C_0}\right]F'' + \left\{\left(\frac{a}{b}\right)^4\frac{D_2}{D_1}\frac{C_2}{C_0} - \left(\frac{a}{b}\right)^2\frac{a^2N_y}{D_1}\frac{C_3}{C_0} + \frac{a^4K}{bD_1C_0}\left[Y^2\left(\frac{1}{2}\right) + Y^2\left(-\frac{1}{2}\right)\right]\right\}F - \frac{a^4\bar{p}}{D_1C_0} = 0 \quad \text{(A6)}$$

and the corresponding boundary conditions at $\xi = 0, 1$ is

$$\left.\begin{aligned} &F'' + \mu_y\left(\frac{a}{b}\right)^2\frac{C_1}{C_0}F = 0 \quad \text{or} \quad \delta F' = 0\\ &F''' - \left[2\left(\frac{a}{b}\right)^2\frac{D_{xy}}{D_1}\frac{C_3}{C_0} - \frac{a^2N_x}{D_1} - \mu_y\left(\frac{a}{b}\right)^2\frac{C_1}{C_0}\right]F' = 0 \quad \text{or} \quad \delta F = 0 \end{aligned}\right\} \quad \text{(A7)}$$

Note that simply supported or clamped edges are permissible boundary conditions on F.

Although Eq. (A6) was derived from static considerations only, it may also be applied to dynamic problems upon proper substitution for the lateral loading. For supersonic flow at Mach number M in the x direction, the following aerodynamic and inertia loadings are substituted for p (where the aerodynamic loading is that given by the two-dimensional static approximation)

$$p = -\frac{2q}{\beta}\frac{\partial w}{\partial x} - \gamma\frac{\partial^2 w}{\partial t^2} \quad \text{(A8)}$$

where q is the dynamic pressure of the flow, γ the panel mass per unit area, and $\beta = (M^2 - 1)^{1/2}$. Then, assuming the deflection as

$$w = Y(\eta)F(\xi)e^{i\omega t} \quad \text{(A9)}$$

where the frequency ω is real for harmonic motion and complex for flutter, the differential equation (A6) can be written as

$$F^{IV} + \pi^2\bar{A}F'' + \lambda F' - \pi^4\bar{B}F = 0 \quad \text{(A10)}$$

for

$$\left.\begin{aligned}\bar{A} &= \frac{a^2N_x}{\pi^2D_1} - 2\left(\frac{a}{b}\right)^2\frac{D_{xy}}{D_1}\left(\frac{C_3}{\pi^2C_0}\right) + 2\mu_y\left(\frac{a}{b}\right)^2\times\\ &\qquad\left(\frac{C_1}{\pi^2C_0}\right)\\ \bar{B} &= \left(\frac{a}{b}\right)^2\left[\frac{a^2N_y}{\pi^2D_1}\left(\frac{C_3}{\pi^2C_0}\right) - \left(\frac{a}{b}\right)^2\frac{D_2}{D_1}\left(\frac{C_2}{\pi^2C_0}\right)\right] +\\ &\qquad\left(\frac{\omega}{\omega_r}\right)^2 - \frac{a^4K}{\pi^4bD_1C_0}\left[Y^2\left(\frac{1}{2}\right) + Y^2\left(-\frac{1}{2}\right)\right]\\ \lambda &= 2qa^3/\beta D_1\\ \omega_r^2 &= \pi^4D_1/\gamma a^4\end{aligned}\right\} \quad (A11)$$

It should be noted that the governing differential equation (A10) is identical to that obtained by Hedgepeth[7] for simply supported isotropic panels. Therefore, the exact solution obtained therein for simply supported leading and trailing edges is applicable to Eq. (A10), and the results of this solution are used directly in the text to show the effect of deflectional spring supports on the flutter characteristics for assumed modes $Y(\eta)$, derived in Appendix B, corresponding to the exact vibration modes.

Appendix B: Vibration Analysis of Simply Supported Panel on Deflectional Springs

In this Appendix the exact vibration analysis is presented for an orthotropic panel simply supported on two opposite edges and elastically supported by deflectional springs of stiffness K on the other two edges. The panel and the coordinate system are shown in Fig. 5c. Neglecting in-plane loads, the differential equation from small-deflection theory governing vibrations of the orthotropic panel is[33]:

$$D_1\frac{\partial^4w}{\partial x^4} + 2(D_{xy} + \mu_xD_2)\frac{\partial^4w}{\partial x^2\partial y^2} + D_2\frac{\partial^4w}{\partial y^4} + \gamma\frac{\partial^2w}{\partial t^2} = 0 \quad (B1)$$

Solution to Eq. (B1) must satisfy the following boundary conditions:

$$w(0, y, t) = w(a, y, t) = w_{,xx}(0, y, t) = w_{,xx}(a, y, t) = 0 \quad (B2)$$

$$(w_{,yy} + \mu_xw_{,xx})_{y=\pm b/2} = 0 \quad (B3)$$

$$[\mp Kw - (2D_{xy} + \mu_xD_2)w_{,xxy} - D_2w_{,yyy}]_{y=\pm b/2} = 0 \quad (B4)$$

where the subscripts comma followed by x or y denote differentiation with respect to the indicated subscript. Equation (B4) accounts for Kirchoff's shear along the edges $y = \pm b/2$.

For simple harmonic motion, a solution to Eq. (B1) is taken in the form

$$w = \sum_m Y_m(\eta)\sin\frac{m\pi x}{a}e^{i\omega t} \quad (B5)$$

where $\eta = y/b$. Eq. (B5) satisfies, term by term, the boundary conditions of Eqs. (B2). We seek then the function $Y_m(\eta)$ which will satisfy the boundary conditions (B3) and (B4). Substituting Eq. (B5) into Eqs. (B1, B3, and B4) results in the following differential equation and boundary conditions on $Y_m(\eta)$:

$$Y_m{}^{IV} - 2\left(\frac{m\pi b}{a}\right)^2\left(\frac{D_{xy}}{D_2} + \mu_x\right)Y_m'' + \left(\frac{\pi b}{a}\right)^4\frac{D_1}{D_2}\left[m^4 - \left(\frac{\omega}{\omega_r}\right)^2\right]Y_m = 0 \quad (B6)$$

$$\left[Y_m'' - \mu_x\left(\frac{m\pi b}{a}\right)^2Y_m\right]_{\eta=\pm1/2} = 0 \quad (B7)$$

$$\left[Y_m''' - \left(2\frac{D_{xy}}{D_2} + \mu_x\right)\left(\frac{m\pi b}{a}\right)^2Y_m' \pm \frac{Kb^3}{D_2}Y_m\right]_{\eta=\pm1/2} = 0 \quad (B8)$$

where $\omega_r^2 = \pi^4D_1/\gamma a^4$ is the fundamental frequency of a beam. The characteristic equation of (B6) is

$$R^4 - 2\pi^2r_1R^2 - \pi^4r_2 = 0 \quad (B9)$$

from which the roots of R become

$$R^2 = \pi^2[r_1 \pm (r_1^2 + r_2)^{1/2}] \quad (B10)$$

where

$$\left.\begin{aligned}r_1 &= \left(\frac{mb}{a}\right)^2\left(\frac{D_{xy}}{D_2} + \mu_x\right)\\ r_2 &= \left(\frac{b}{a}\right)^4\frac{D_1}{D_2}\left[\left(\frac{\omega}{\omega_r}\right)^2 - m^4\right]\end{aligned}\right\} \quad (B11)$$

It can be shown that $r_2 \geqq 0$ and r_1 is always positive. Thus, from Eq. (B10) the roots are either real or purely imaginary. Then, considering only even functions of Y_m yields the following solution to Eq. (B6):

$$Y_m = A_m\cosh\alpha\pi\eta + B_m\cos\epsilon\pi\eta \quad (B12)$$

where

$$\left.\begin{aligned}\alpha^2 &= r_1 + (r_1^2 + r_2)^{1/2}\\ \epsilon^2 &= -r_1 + (r_1^2 + r_2)^{1/2}\end{aligned}\right\} \quad (B13)$$

Upon substitution of Eq. (B12) into the boundary conditions on Y_m [Eqs. (B7) and (B8)], a nontrivial solution requires that the determinant of the coefficients of A_m and B_m be zero; this gives the following transcendental equation:

$$\epsilon(\epsilon^2 + \psi)^2\tan\epsilon\frac{\pi}{2} + \alpha(\alpha^2 - \psi)^2\tanh\alpha\frac{\pi}{2} - \bar{K}(\alpha^2 + \epsilon^2) = 0 \quad (B14)$$

where

$$\left.\begin{aligned}\bar{K} &= \frac{K}{D_2}\left(\frac{b}{\pi}\right)^3\\ \psi &= \left(\frac{mb}{a}\right)^2\left(2\frac{D_{xy}}{D_2} + \mu_x\right)\end{aligned}\right\} \quad (B15)$$

Equation (B14) is solved for the roots α and ϵ for known values of the parameter r_1 and spring stiffness parameter $\bar{K}$. Solutions to Eq. (B14) (for $\mu_x = 0$) are shown in Fig. 6 and discussed in the text. For each root of α and ϵ, the corresponding mode shape Y_m is

$$Y_m(\eta) = B_m(\cos\epsilon\pi\eta + \varphi\cosh\alpha\pi\eta) \quad (B16)$$

where

$$\varphi = \frac{\left[\epsilon^2 + \mu_x\left(\frac{mb}{a}\right)^2\right]}{\left[\alpha^2 - \mu_x\left(\frac{mb}{a}\right)^2\right]}\frac{\cos\epsilon\frac{\pi}{2}}{\cosh\alpha\frac{\pi}{2}} \quad (B17)$$

Equation (B16) is employed in the text to show the effects of deflectional spring stiffness on flutter predictions of orthotropic panels.

References

[1] Sylvester, M. A. and Baker, J. E., "Some experimental studies of panel flutter at Mach number 1.3," NACA TN 3914 (1957).

[2] Sylvester, M. A., "Experimental studies of flutter of buckled rectangular panels at Mach numbers from 1.2 to 3.0 including effects of pressure differential and of panel width-length ratio," NASA TN D-833 (1961).

[3] Miles, J. W., "On the aerodynamic instability of thin panels," J. Aeronaut. Sci. **23**, 771–780 (1956).

[4] Hedgepeth, J. M., Budiansky, B., and Leonard, R. W., "Analysis of flutter in compressible flow of a panel on many supports," J. Aeronaut. Sci. **21**, 475–486 (1954).

[5] Luke, Y. L., St. John, A. D., and Goland, M., "An exact solution for two-dimensional linear panel flutter at supersonic speeds," Midwest Research Institute, Wright Air Development Center TN 56-466, Contract AF33(616)-2867 (March 15, 1956).

[6] Nelson, H. C. and Cunningham, H. J., "Theoretical investigation of flutter of two-dimensional flat panels with one surface exposed to supersonic potential flow," NACA Rept. 1280 (1956).

[7] Hedgepeth, J. M., "Flutter of rectangular simply supported panels at high supersonic speeds," J. Aeronaut. Sci. **24**, 563–573, 586 (1957).

[8] Fung, Y. C. B., "A summary of the theories and experiments on panel flutter," Air Force Office of Scientific Res. TN 60-224, Graduate Astronautical Laboratory, California Institute of Technology (May 1960).

[9] Stocker, J. E., "A comprehensive review of theoretical and experimental panel flutter investigations," North American Aviation, Inc., Columbus Division, Rept. NA 61H-444 (September 15, 1961).

[10] Kordes, E. E., Tuovila, W. J., and Guy, L. D., Flutter research on skin panels," NASA TN D-451 (1960).

[11] Bohon, H. L., "Panel flutter tests on full-scale X-15 lower vertical stabilizer at Mach number of 3.0," NASA TN D-1385 (1962).

[12] Kordes, E. E. and Noll, R. B., "Flight flutter results for flat rectangular panels," NASA TN D-1058 (1962).

[13] McElman, J. A., "Flutter of curved and flat sandwich panels subjected to supersonic flow," NASA TN D-2192 (1964).

[14] Kordes, E. E. and Noll, R. B., "Theoretical flutter analysis of flat rectangular panels in uniform coplanar flow with arbitrary direction," NASA TN D-1156 (1962).

[15] Eisley, J. G. and Luessen, G., "The flutter of thin plates under combined shear and normal edge forces including the effects of varying sweepback," IAS Paper 62-90 (June 1962).

[16] Bohon, H. L., "Flutter of flat rectangular orthotropic panels with biaxia loading and arbitrary flow direction," NASA TN D-1949 (1963).

[17] Dixon, S. C., Griffith, G. E., and Bohon, H. L., "Experimental investigation at Mach number 3.0 of the effects of thermal stress and buckling on the flutter of four-bay aluminum-alloy panels with length-width ratios of 10," NASA TN D-921 (1961).

[18] Dixon, S. C., "Experimental investigation at Mach number 3.0 of effects of thermal stress and buckling on flutter characteristics of flat single-bay panels of length-width ratio 0.96," NASA TN D-1485 (1962).

[19] Dixon, S. C., "Application of transtability concept to flutter of finite panels and experimental results," NASA TN D-1948 (1963).

[20] Dixon, S. C. and Shore, C. P., "Effects of differential pressure, thermal stress, and buckling on flutter of flat panels with length-width ratio of 2," NASA TN D-2047 (1963).

[21] Guy, L. D. and Bohon, H. L., "Flutter of aerodynamically heated aluminum-alloy and stainless-steel panels with length-width ratio of 10 at Mach number of 3.0," NASA TN D-1353 (1962).

[22] Fralich, R. W., "Postbuckling effects on the flutter of simply supported rectangular panels at supersonic speeds," NASA TN D-1615 (1963).

[23] Voss, H. M., "The effect of some practical complications on the flutter of rectangular panels," *Symposium Proceedings, Structural Dynamics of High-Speed Flight, ACR-62* (Aircraft Industries Association and Office Naval Research, April 1961), Vol. 1, pp. 252–267.

[24] Johns, D. J. and Parks, P. C., "Effect of structural damping on panel flutter," Aircraft Eng. **32**, 304–308 (October 1960).

[25] Guy, L. D. and Dixon, S. C., "A critical review of experiment and theory for flutter of aerodynamically heated panels," *Symposium on Dynamics of Manned Lifting P ane ary Entry*, edited by S. M. Scala, A. C. Harrison, and M. Rodgers (John Wiley & Sons, Inc., New York, 1963), pp. 568–595.

[26] Bohon, H. L., "Experimental flutter results for corrugation-stiffened panels at a Mach number of 3," NASA TN D-2293 (1964).

[27] Cunningham, H. J., "Flutter analysis of flat rectangular panels based on three-dimensional supersonic potential flow," AIAA J. **1**, 1795–1801 (1963).

[28] McClure, J. D., "Stability of finite chord panels exposed to low supersonic flows with a turbulent boundary layer," IAS Paper 63-21 (1963).

[29] Fung, Y. C., "Some recent contributions to panel flutter research," IAS Paper 63–26 (1963).

[30] Houbolt, J. C., *A Study of Several Aerothermoelastic Problems of Aircraft Structures in High-Speed Flight* (Nr. 5 Mitteilunger aus dem Institut für Flugzeugstatik und Leichtbau, Leeman, Zürich, 1958).

[31] Movchan, A. A., "On the stability of a panel moving in a gas," NASA RE 11-21-58W (1959).

[32] Pride, R. A., Royster, D. M., and Helms, B. F., "Design, test, and analysis of a hot structure for lifting reentry vehicles," NASA TN D-2186 (1964).

[33] Stroud, W. J., "Elastic constants for bending and twisting of corrugation-stiffened panels," NASA TR R-166 (1963).

[34] Kantorovich, L. V. and Krylov, V. I., *Approximate Methods of Higher Analysis* (Interscience Publishers, Inc., New York, 1958), pp. 304–308.

[35] Libove, C. and Batdorf, S. B., "A general small-deflection theory for flat sandwich plates," NACA Rept. 899 (1948).